JOURNAL OF MATERIALS SCIENCE 35 (2000) 5283–5289

# Stability of $SrZr_{0.9}Yb_{0.1}O_{3-\alpha}$ protonic conductor in atmosphere containing nitrogen oxides ($NO_x$)

T. KOBAYASHI, S. MORISHITA, T. HONMA, K. ABE, Y. UKYO
*Toyota Central R&D Labs., Inc., Nagakute, Aichi, 480-1192 Japan*
*E-mail: tetsuro@mosk.tytlabs.co.jp*

H. IWAHARA
*Center for Integrated Research in Science and Engineering, Nagoya University, Furo-cho, Chikusa-ku, Nagoya, 464-8603 Japan*

The stability of the $SrZr_{0.9}Yb_{0.1}O_{3-\alpha}$ protonic conductor in an atmosphere containing nitrogen oxides ($NO_x$) was investigated. When a fine powder of $SrZr_{0.9}Yb_{0.1}O_{3-\alpha}$ with a specific surface area of about 50 $m^2/g$ was annealed at 440 °C in He gas containing 8% $O_2$ and 0.1% NO, the formation of $Sr(NO_3)_2$ was observed by IR measurement, ion-chromatography analysis and ICP analysis. The formation mechanism of $Sr(NO_3)_2$ was examined by considering the thermodynamic equilibrium. Based on the results of the thermodynamic calculation, $H_2O$ dissolved into $SrZr_{0.9}Yb_{0.1}O_{3-\alpha}$ was estimated to play an important role in the reaction for the formation of $Sr(NO_3)_2$ between $SrZr_{0.9}Yb_{0.1}O_{3-\alpha}$ and $NO_x$. 

## 1. Introduction

$SrCe_{0.95}Yb_{0.05}O_{3-\alpha}$, $BaCe_{0.8}Gd_{0.2}O_{3-\alpha}$ and $SrZr_{0.9}Yb_{0.1}O_{3-\alpha}$ ($\alpha$: mole fraction of oxide ion vacancies) with the perovskite-type structure have oxide ion vacancies, and $H_2O$ can be dissolved into the crystal structure according to Equation 1,

$$H_2O + V_O^{\bullet\bullet} \rightleftarrows 2H^{\bullet} + O_O^{\times} \quad (1)$$

where $V_O^{\bullet\bullet}$ is the oxide ion vacancy, $H^{\bullet}$ is the proton and $O_O^{\times}$ is the oxide ion at the normal lattice site [1, 2]. $H_2O$ dissolved in the perovskite structure forms protons combined with oxide ions at the normal lattice sites by an OH bond [3]. This proton can migrate around semistable positions near the oxide ion by the hopping conduction mechanism [4] and shows high protonic mobility ($5 \times 10^{-5}$ ($cm^2\,s^{-1}\,V^{-1}$)) around 700 °C [5].

These materials have been widely studied for their applications to hydrogen sensors [6–10], SOFCs [11–15] and gas reactors [16–18] by utilizing their protonic conduction. On the other hand, we constructed a steam electrolysis cell using this protonic conductor as an electrolyte and proposed a new method of NO reduction using the electrolysis cell [19]. This method allows harmful nitrogen oxides in the exhaust gases from combustion engines to be reduced using hydrogen produced by the electrolysis of steam that is also contained in the exhaust gases [19].

The study on the chemical stability of these protonic conductors is necessary for the application of these devices. Taniguchi *et al.* have examined the stability of the protonic conductor, $BaCe_{0.8}Gd_{0.2}O_{3-\alpha}$, in an atmosphere containing $CO_2$ using TG and XRD measurements [20]. They have reported that $BaCe_{0.8}Gd_{0.2}O_{3-\alpha}$ is stable when the $CO_2$ concentration is less than 15%, however, it is decomposed into barium carbonate and fluorite-type cerium gadolinium oxide in an atmosphere containing more than 18% $CO_2$ at a temperature higher than 500 °C. Scholten *et al.* have studied the reaction of protonic conductors based on $SrCeO_3$, $BaCeO_3$, $SrZrO_3$ and $BaZrO_3$ with $CO_2$ by calculating the thermodynamic equilibrium [21, 22]. Kreuer has summarized the stability of protonic conductors in an atmosphere containing $CO_2$ or $H_2O$ [23], and mentioned the relation between the thermodynamic stability and conductivity of protonic conductors [24].

In this paper, the chemical stability of $SrZr_{0.9}Yb_{0.1}O_{3-\alpha}$ in an atmosphere containing $NO_x$ was investigated. Fine $SrZr_{0.9}Yb_{0.1}O_{3-\alpha}$ powder with a specific surface area of about 50 $m^2/g$ was prepared, and annealed in an atmosphere containing $NO_x$, and then the reaction products were analyzed. Moreover, the stability of $SrZrO_3$ was examined by calculating the thermodynamic equilibrium, and the reaction mechanism between $SrZr_{0.9}Yb_{0.1}O_{3-\alpha}$ and $NO_x$ was estimated using these calculations.

## 2. Experimental procedure

$SrCO_3$ powder (Rare Metallic Co., Ltd., 4N), $ZrO_2$ powder (Rare Metallic Co., Ltd., 4N) and $Yb_2O_3$ powder (Kojundo Chemical Lab. Co., Ltd., 4N) were used as the starting materials for the synthesis of the $SrZr_{0.9}Yb_{0.1}O_{3-\alpha}$ powder. These powders were well mixed in the desired proportion of $SrZr_{0.9}Yb_{0.1}O_3$ by ball-milling for 3 days. The mixed powder was then calcined in air at 1350 °C for 10 hours. By XRD measurement, it was revealed that the calcined powder

had an orthorhombic perovskite-type structure, i.e., $SrZr_{0.9}Yb_{0.1}O_{3-\alpha}$, and no additional phases were detected. The specific surface area of the powder was about 3 $m^2/g$. Fine $SrZr_{0.9}Yb_{0.1}O_{3-\alpha}$ powder with a specific surface area of about 50 $m^2/g$ was then obtained by ball-milling the calcined powder for 7 days. The ground powder was also $SrZr_{0.9}Yb_{0.1}O_{3-\alpha}$ single phase.

The annealing of $SrZr_{0.9}Yb_{0.1}O_{3-\alpha}$ was carried out at 440 °C in He gas containing 8% $O_2$ and 0.1% NO. The annealing temperature and the concentration of $O_2$ and NO corresponded to those of the exhaust gases from automobile engines operated under lean-burn conditions of which the ratio of air to fuel was about 20.

Fig. 1 shows the schematic diagram of the annealing experiment for the fine $SrZr_{0.9}Yb_{0.1}O_{3-\alpha}$ powder. Sample (a) was the fine $SrZr_{0.9}Yb_{0.1}O_{3-\alpha}$ powder annealed at 800 °C in air for 3 hours. Sample (b) was the fine $SrZr_{0.9}Yb_{0.1}O_{3-\alpha}$ powder heated from room temperature to 440 °C in He gas, and annealed at 440 °C in He gas containing 8% $O_2$ and 0.1% NO for 4.5 hours, and then cooled from 440 °C to room temperature in He gas. Sample (c) was obtained by the same process as sample (b) except that the annealing time was 36 hours. In order to prevent the absorption of $NO_x$ between room temperature and 440 °C, pure He gas was used during the heating and cooling.

Samples (a), (b) and (c) were analyzed by XRD and FT-IR measurements to investigate the reaction during annealing. Furthermore, 150 mg of sample (a) or (c) was added to 20 ml of the ultrapure water and stirred for 30 minutes, and then the dissolved ions were analyzed. The negative and positive ions were determined by ion-chromatography and ICP analysis, respectively.

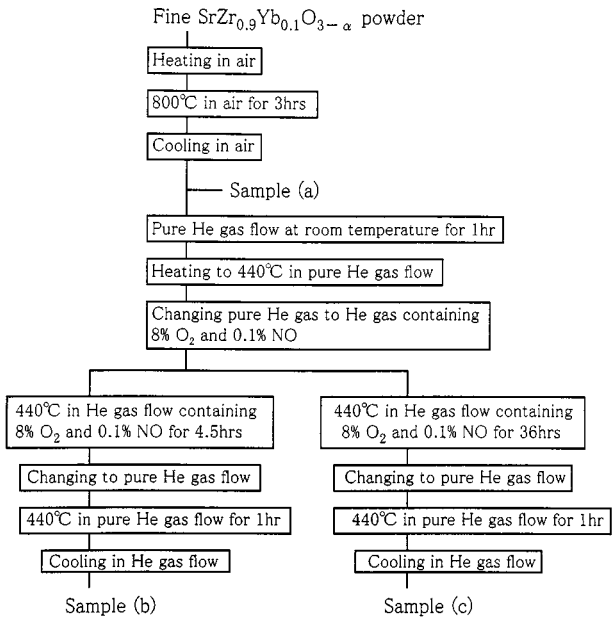


*Figure 1* The experimental procedure of annealing $SrZr_{0.9}Yb_{0.1}O_{3-\alpha}$ in air and in He containing 8% $O_2$ and 0.1% NO.

## 3. Result and discussion

### 3.1. Annealing in the atmosphere containing NO and $O_2$

Fig. 2 shows XRD pattern of sample (c). The XRD pattern showed only the peaks of $SrZrO_3$ with the orthorhombic perovskite-type structure.

Fig. 3 shows the IR profiles of samples (a), (b) and (c). The absorption peaks for $CO_3^{2-}$ were detected around 850 $cm^{-1}$ and 1470 $cm^{-1}$ in all samples. These show the possibility that the fine $SrZr_{0.9}Yb_{0.1}O_{3-\alpha}$ powder reacted with $CO_2$ in air. The absorption peak for $NO_3^-$ was detected around 1380 $cm^{-1}$ for samples (b) and (c) which were annealed at 440 °C in He gas containing NO and $O_2$. It shows the possibility that $NO_3^-$ was formed by the reaction of the $SrZr_{0.9}Yb_{0.1}O_{3-\alpha}$ powder with NO and $O_2$, because the intensity of the $NO_3^-$-absorption peak of sample (c), which was annealed for 36 hours, is stronger than that of sample (b) annealed for 4.5 hours.

Table I shows the concentrations of ions dissolved in water for samples (a) and (c). The amount of $Sr^{2+}$ and $NO_3^-$ ions dissolved from sample (c) are very large

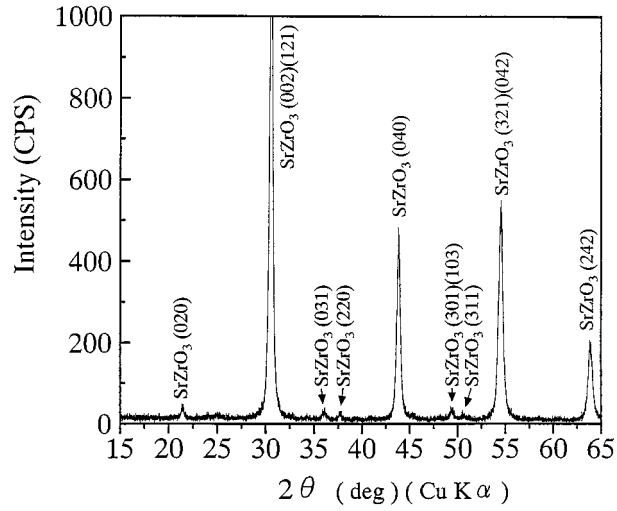


*Figure 2* XRD pattern of sample (c) annealed in He containing 8% $O_2$ and 0.1% NO at 440 °C for 36 hrs.

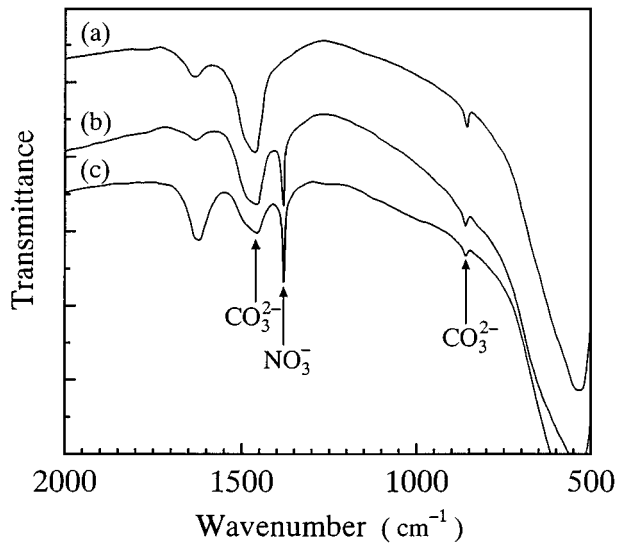


*Figure 3* IR profiles of samples (a), (b) and (c); (a) is annealed in air at 800 °C for 3 hrs, (b) is annealed in 8% $O_2$ and 0.1% NO at 440 °C for 4.5 hrs, and (c) is annealed in 8% $O_2$ and 0.1% NO at 440 °C for 36 hrs.

TABLE I Concentrations of ions dissolved in water from samples (a) and (c)

| Ion | Sample (a) (mol $l^{-1}$) | Sample (c) (mol $l^{-1}$) |
|---|---|---|
| $Sr^{2+}$ | $2.7_4 \times 10^{-5}$ | $2.7_4 \times 10^{-4}$ |
| $Yb^{3+}$ | $<5.7_8 \times 10^{-8}$ | $<5.7_8 \times 10^{-8}$ |
| $Zr^{4+}$ | $8.7_7 \times 10^{-7}$ | $<1.1_0 \times 10^{-7}$ |
| $NO_2^-$ | $4.9_0 \times 10^{-7}$ | $1.1_1 \times 10^{-5}$ |
| $NO_3^-$ | $4.8_5 \times 10^{-7}$ | $3.7_9 \times 10^{-4}$ |

TABLE II The list of the standard molar enthalpy and entropy of formations.

| Compound | $\Delta H_f^\circ$ (kJ $mol^{-1}$) | $\Delta S_f^\circ$ (J $K^{-1}$ $mol^{-1}$) |
|---|---|---|
| $CO_2$ (gas) | −393.51 | 213.63 |
| $H_2$ (gas) | 0.0 | 130.575 |
| $H_2O$ (gas) | −241.818 | 188.716 |
| NO (gas) | 90.25 | 210.65 |
| $NO_2$ (gas) | 33.18 | 239.95 |
| $O_2$ (gas) | 0.0 | 205.03 |
| $SrCO_3$ (solid) | −1220.1 | 97.1 |
| $Sr(NO_3)_2$ (solid) | −978.22 | 194.56 |
| $SrZrO_3$ (solid) | −1767.30 | 115.10 |
| $ZrO_2$ (solid) | −1100.56 | 50.38 |

compared with that from sample (a). This means that the product during the annealing of $SrZr_{0.9}Yb_{0.1}O_{3-\alpha}$ is considered to be $Sr(NO_3)_2$.

## 3.2. Thermodynamic equilibrium calculation

The formation reaction of $Sr(NO_3)_2$ described above was estimated by calculating the thermodynamic equilibrium. The thermodynamic parameters listed in Table II were used for the calculation. The parameters for $SrZrO_3$ instead of for $SrZr_{0.9}Yb_{0.1}O_{3-\alpha}$ were used, because there was no references for the thermodynamic data for $SrZr_{0.9}Yb_{0.1}O_{3-\alpha}$.

### *3.2.1. Reaction of $SrZrO_3$ with $CO_2$*

Calculation for the formation reaction of $CO_3^{2-}$ was attempted first. By considering the equilibrium of Equation 2, the partial pressure of $CO_2$ ($P_{CO2}$) in an equilibrium state can be calculated.

$$SrZrO_3 + CO_2 \rightleftarrows SrCO_3 + ZrO_2 \tag{2}$$

The change in enthalpy ($\Delta H_r^\circ$), entropy ($\Delta S_r^\circ$) and standard Gibbs energy ($\Delta G_r^\circ$) of formation of $SrCO_3$ and $ZrO_2$ from $SrZrO_3$ and $CO_2$ are calculated as follows.

$$\begin{aligned}&\Delta H_r^\circ(298.15)\ (\mathrm{kJ\,mol^{-1}})\\ &\quad = -1220.1 - 1100.56 + 1767.30 + 393.51\\ &\quad = -159.85 \qquad (3)\\ &\Delta S_r^\circ(298.15)\ (\mathrm{J\,K^{-1}\,mol^{-1}})\\ &\quad = 97.1 + 50.38 - 115.10 - 213.63\\ &\quad = -181.25 \qquad (4)\end{aligned}$$

$$\begin{aligned}&\Delta G_r^\circ(T)\ (\mathrm{J\,mol^{-1}})\\ &\quad = \Delta H_r^\circ(T)\ (\mathrm{J\,mol^{-1}}) - T \times \Delta S_r^\circ(T)\ (\mathrm{J\,K^{-1}\,mol^{-1}})\\ &\quad \cong \Delta H_r^\circ(298.15)\ (\mathrm{J\,mol^{-1}})\\ &\qquad - T \times \Delta S_r^\circ(298.15)\ (\mathrm{J\,K^{-1}\,mol^{-1}})\\ &\quad \cong -159.85 \times 10^3 + 181.25 \times T \qquad (5)\end{aligned}$$

When reaction (2) is in an equilibrium state, the difference in the chemical potential of the left and right sides of Equation 2 is zero.

$$\begin{aligned}\Delta G(T) &= \mu_{SrCO3} + \mu_{ZrO2} - \mu_{SrZrO3} - \mu_{CO2} = 0\\ &= \mu^\circ_{SrCO3} + \mu^\circ_{ZrO2} - \mu^\circ_{SrZrO3} - \mu^\circ_{CO2}\\ &\quad + RT \ln(a_{SrCO3}a_{ZrO2}/a_{SrZrO3})\\ &\quad - RT \ln a_{CO2}\\ &\cong \Delta G_r^\circ(T) - RT \ln P_{CO2} = 0 \qquad (6)\end{aligned}$$

The activities of $SrZrO_3$, $Sr(NO_3)_2$ and $ZrO_2$ should be unity, because they are solid phases.

$$a_{SrCO3}a_{ZrO2}/a_{SrZrO3} \cong 1 \tag{7}$$

The activity of $CO_2$ can be expressed by the partial pressure of $CO_2$.

$$a_{CO2} \cong P_{CO2} \tag{8}$$

Equation 9 is derived from Equations 5–8.

$$\mathrm{Log}\ P_{CO2} = 9.47 - 8.35 \times 10^3/T \tag{9}$$

Fig. 4 shows the relation between Log $P_{CO2}$ and $1/T$ according to Equation 9. This result is in good agreement with that obtained by Scholten *et al.* [21] or by Kreuer [23]. $SrCO_3$ and $ZrO_2$ are thermodynamically stable in the upper right region of the line indicated by Equation 9, $SrZrO_3$ and $CO_2$ are stable in the bottom

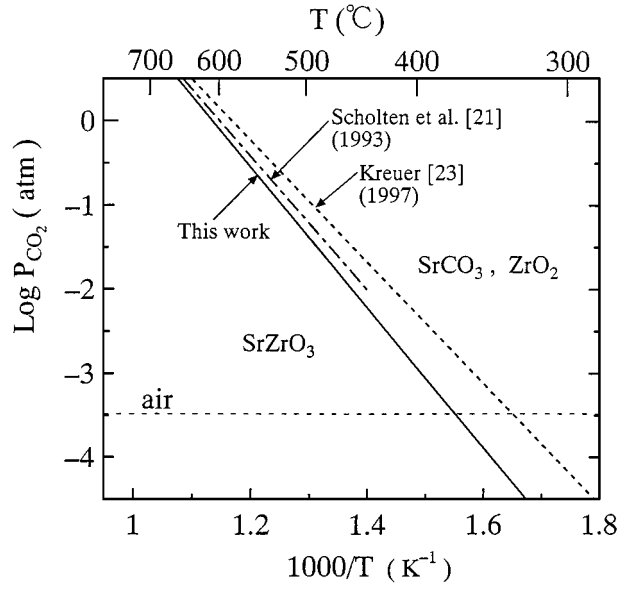


*Figure 4* Stability of $SrZrO_3$ in atmosphere containing $CO_2$.

left. Because the partial pressure of $CO_2$ in air is about $10^{-3.5}$, the mixture of $SrCO_3$ and $ZrO_2$ is more thermodynamically stable than the mixture of $SrZrO_3$ and $CO_2$ at temperatures lower than 370 °C. The existence of $CO_3^{2-}$ shown in Fig. 3 indicates the formation of $SrCO_3$ by the reaction of fine $SrZr_{0.9}Yb_{0.1}O_{3-\alpha}$ powder with $CO_2$ in air before and after the $NO_x$-annealing. This reaction rate might depend on the characteristics of the samples. The specific surface area of the $SrZr_{0.9}Yb_{0.1}O_{3-\alpha}$ powder used in this study is about 50 $m^2/g$ so that the reaction rate with $CO_2$ might be comparatively fast. However, it was postulated that the reaction rate of the sintered $SrZr_{0.9}Yb_{0.1}O_{3-\alpha}$ with $CO_2$ might be slow, therefore, it can be used as the electrolyte of a steam electrolysis cell.

### 3.2.2. Reaction of $SrZrO_3$ with $NO_x$

The formation reaction of $NO_3^-$ can be dealt with using the same method described above.

When NO is mixed with $O_2$, $NO_2$ must be produced according to Equation 10.

$$1/2O_2 + NO \rightleftarrows NO_2 \quad (10)$$

Fig. 5 shows the existence ratio of $NO_2$ to the sum of NO and $NO_2$ calculated by the equilibrium constant at a constant pressure in He containing 8% $O_2$ and 0.1% NO. When this gas is in an equilibrium state at 440 °C, the concentrations of NO and $NO_2$ are calculated to be 0.016% and 0.084%, respectively. In this experiment, however, the gas used for annealing is not thought to be in the equilibrium state, therefore, we dealt with the two reactions between $SrZrO_3$ and NO, and between $SrZrO_3$ and $NO_2$. The experimental conditions were assumed such that the concentrations of NO and $NO_2$ are less than 0.1%, respectively.

An oxygen source must be necessary for the formation of $Sr(NO_3)_2$ by the reaction of $SrZrO_3$ with NO or $NO_2$.

First, $O_2$ in the gas used for annealing is assumed as the oxygen source.

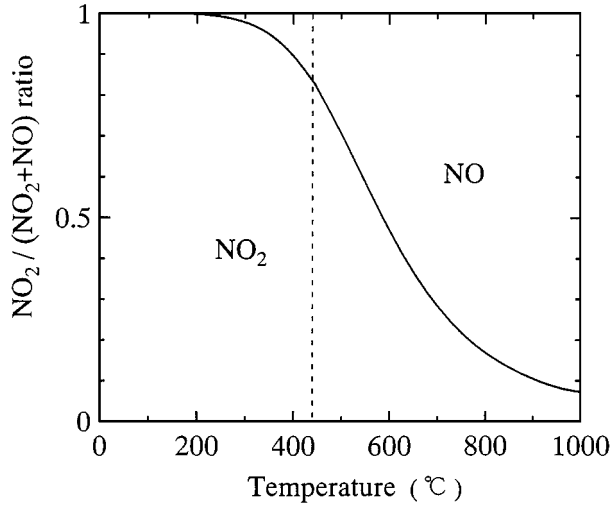


*Figure 5* Phase diagram of $NO_2$-NO system in a gas containing 8% $O_2$ and 0.1% NO. ($NO + 1/2\ O_2 = NO_2$).

The same calculation as described above can be applied for reactions (11) and (13), and Equations 12 and 14 were derived, respectively.

$$SrZrO_3 + 2NO + 3/2O_2 \rightleftarrows Sr(NO_3)_2 + ZrO_2 \quad (11)$$

$$\text{Log } P_{NO} = -3/4 \text{ Log } P_{O2} + 15.65 - 12.85 \times 10^3/T \quad (12)$$

$$SrZrO_3 + 2NO_2 + 1/2O_2 \rightleftarrows Sr(NO_3)_2 + ZrO_2 \quad (13)$$

$$\text{Log } P_{NO2} = -1/4 \text{ Log } P_{O2} + 11.83 - 9.87 \times 10^3/T \quad (14)$$

Equations 15 and 16 are then derived from Equations 12 and 14 when the concentration of $O_2$ in the gas is 8%.

$$\text{Log } P_{NO} = 16.47 - 12.85 \times 10^3/T \quad (15)$$

$$\text{Log } P_{NO2} = 12.10 - 9.87 \times 10^3/T \quad (16)$$

The dependence of $P_{NO}$ and $P_{NO2}$ on the temperature is plotted in Figs 6 and 7 according to (12) and (15), and

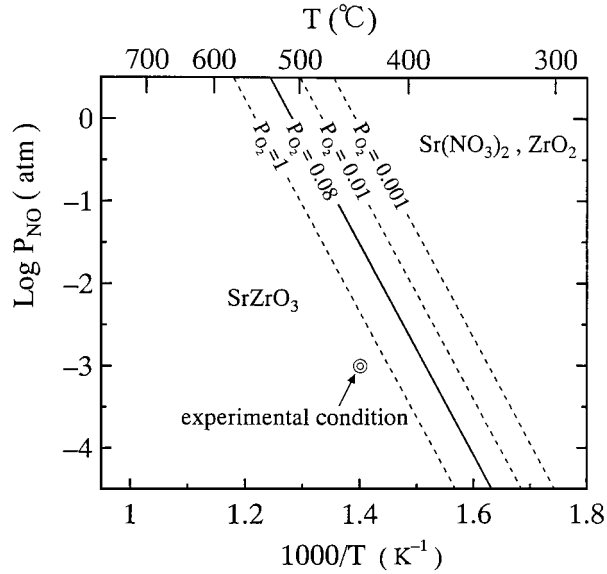


*Figure 6* Stability of $SrZrO_3$ in atmosphere containing NO and $O_2$.

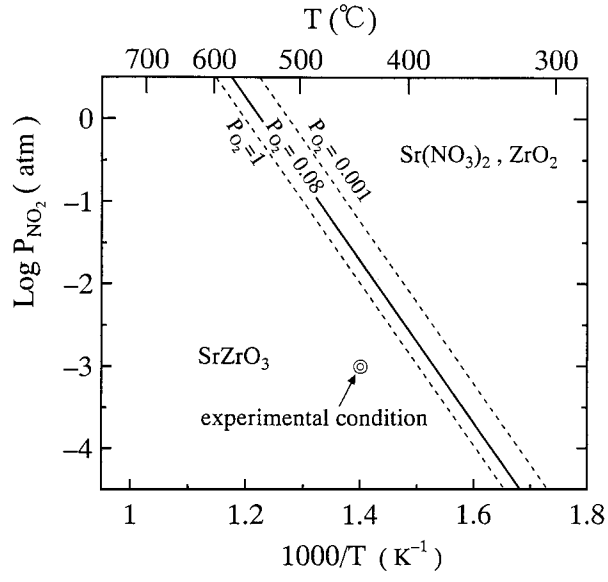


*Figure 7* Stability of $SrZrO_3$ in atmosphere containing $NO_2$ and $O_2$.

(14) and (16), respectively. In Figs 6 and 7, $Sr(NO_3)_2$ and $ZrO_2$ are thermodynamically stable in the upper right region and $SrZrO_3$ is stable in the bottom left. The experimental conditions used in this study are located in the bottom left region of Figs 6 and 7. This shows that $SrZrO_3$ is more stable, and that $Sr(NO_3)_2$ can not be formed by reactions (11) and (13) under these experimental conditions.

Another possibility for the oxygen source for the formation of $Sr(NO_3)_2$ is the oxygen in $H_2O$ dissolved into $SrZrO_3$ (Equation 1). This reaction may be written as Equations 17 and 18.

$$SrZrO_3 + 2NO + 6H^{\bullet} + 3O_O^{\times} \rightleftarrows Sr(NO_3)_2 + ZrO_2 + 3V_O^{\bullet\bullet} + 3H_2 \quad (17)$$

$$SrZrO_3 + 2NO_2 + 2H^{\bullet} + O_O^{\times} \rightleftarrows Sr(NO_3)_2 + ZrO_2 + V_O^{\bullet\bullet} + H_2 \quad (18)$$

$H_2$ gas produced by reactions (17) and (18) may react fast with $O_2$ in the gas phase, and then, they are considered to reach fast the equilibrium state expressed by Equation 19.

$$H_2 + 1/2O_2 \rightleftarrows H_2O \text{ (gas)} \quad (19)$$

Therefore, the total reactions are written as Equations 20 and 21.

$$SrZrO_3 + 2NO + 6H^{\bullet} + 3O_O^{\times} + 3/2O_2 \rightleftarrows Sr(NO_3)_2 + ZrO_2 + 3V_O^{\bullet\bullet} + 3H_2O \text{ (gas)} \quad (20)$$

$$SrZrO_3 + 2NO_2 + 2H^{\bullet} + O_O^{\times} + 1/2O_2 \rightleftarrows Sr(NO_3)_2 + ZrO_2 + V_O^{\bullet\bullet} + H_2O \text{ (gas)} \quad (21)$$

Uchida *et al.* have reported the equilibrium constant $K_3$ of reaction (1) for the dissolution reaction of $H_2O$ into $SrCe_{0.95}Yb_{0.05}O_{3-\alpha}$ [2].

$$H_2O \text{ (gas)} + V_O^{\bullet\bullet} \overset{K_3}{\rightleftarrows} 2H^{\bullet} + O_O^{\times} \quad (1)$$

Their result is shown in Fig. 8. Based on the assumption that $K_3$ was expressed by the straight line (the broken line in Fig. 8) in the temperature range of 600–800 °C, Equation 22 is obtained.

$$\mathrm{Log}_{10} K_3 = 0.0252 + 0.594 \times 10^3/T(K) \quad (22)$$

This $K_3$ value for $SrCe_{0.95}Yb_{0.05}O_{3-\alpha}$ instead of for $SrZr_{0.9}Yb_{0.1}O_{3-\alpha}$ is employed for the calculation of the standard Gibbs energy ($\Delta G_r^{\circ}$) for Equations 20 and 21, because there is no references for $K_3$ value for $SrZr_{0.9}Yb_{0.1}O_{3-\alpha}$. The difference between the equilibrium constants for $SrCe_{0.95}Yb_{0.05}O_{3-\alpha}$ and for $SrZr_{0.9}Yb_{0.1}O_{3-\alpha}$ is thought to be small, because they are protonic conductors and have the perovskite-type structure containing the Sr ion.

Finally, Equations 23 and 24 are obtained for reactions (20) and (21), respectively.

$$\mathrm{Log}\, P_{NO} = 3/2\ \mathrm{Log}\, P_{H2O} - 3/4\ \mathrm{Log}\, P_{O2} + 15.69 - 11.96 \times 10^3/T \quad (23)$$

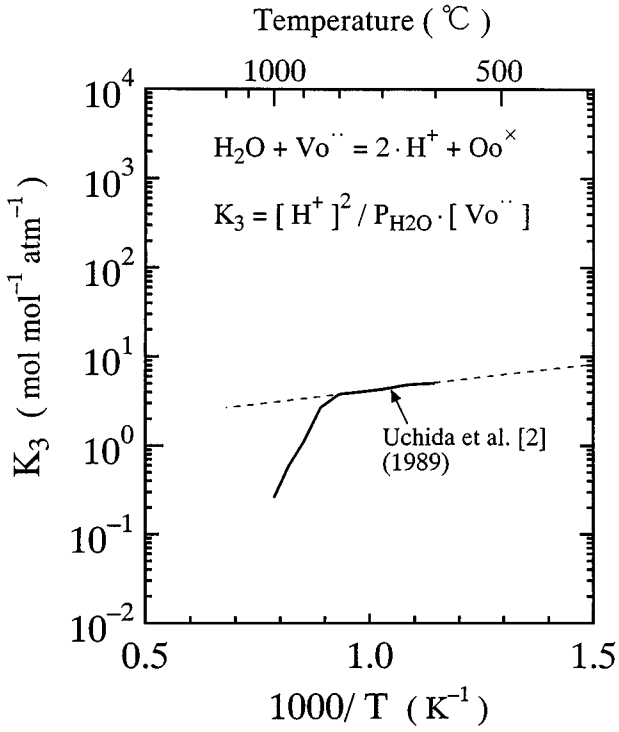


*Figure 8* Equilibrium constant $K_3$ for $SrCe_{0.95}Yb_{0.05}O_{3-\alpha}$.

$$\mathrm{Log}\, P_{NO2} = 1/2\ \mathrm{Log}\, P_{H2O} - 1/4\ \mathrm{Log}\, P_{O2} + 11.84 - 9.57 \times 10^3/T \quad (24)$$

When $P_{O2} = 0.08$ is inserted into Equations 23 and 24, Equations 25 and 26 are obtained.

$$\mathrm{Log}\, P_{NO} = 3/2\ \mathrm{Log}\, P_{H2O} + 16.51 - 11.96 \times 10^3/T \quad (25)$$

$$\mathrm{Log}\, P_{NO2} = 1/2\ \mathrm{Log}\, P_{H2O} + 12.11 - 9.57 \times 10^3/T \quad (26)$$

Equations 25 and 26 are shown in Figs 9 and 10. The concentration of $H_2O$ as an impurity in gases

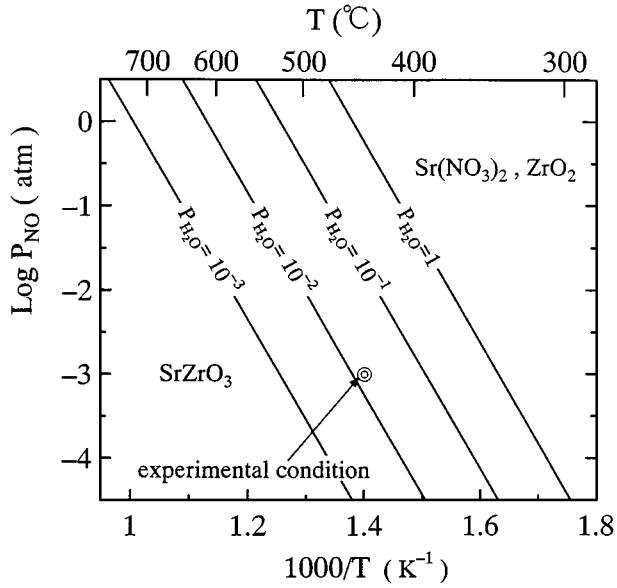


*Figure 9* Stability of $SrZrO_3$ in atmosphere containing NO and 8% $O_2$.

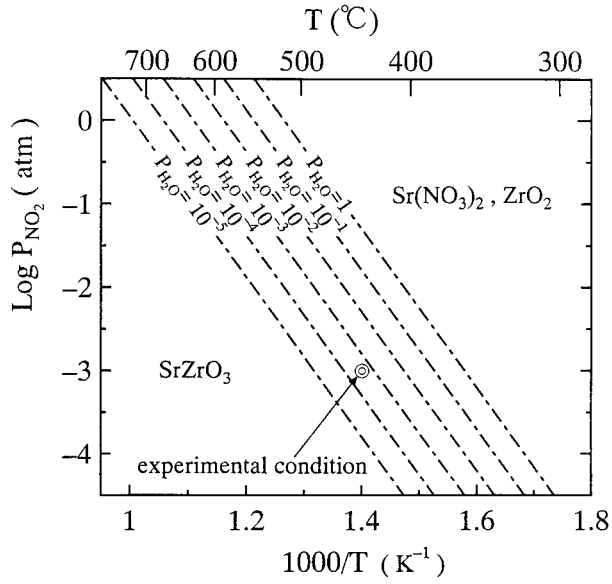


*Figure 10* Stability of $SrZrO_3$ in atmosphere containing $NO_2$ and 8% $O_2$.

used in this experiment was less than 2 ppm, i.e., $P_{H2O} < 2 \times 10^{-6}$, therefore, the experimental conditions fall into the upper right region of Figs 9 and 10 in which $Sr(NO_3)_2$ is stable.

These calculations reveal that the stable region of $SrZrO_3$ spreads out when $P_{H2O}$ is higher. This is because the dissolution of $H_2O$ into $SrZrO_3$ proceeds and the amount of oxygen taking part in the formation of $Sr(NO_3)_2$ decreases with increasing $P_{H2O}$.

In the above calculation, the thermodynamic parameters for $SrZrO_3$ instead of for $SrZr_{0.9}Yb_{0.1}O_{3-\alpha}$ have been used. However, the difference between these parameters for $SrZrO_3$ and for $SrZr_{0.9}Yb_{0.1}O_{3-\alpha}$ is considered to be very small. Therefore, $H_2O$ dissolved into $SrZr_{0.9}Yb_{0.1}O_{3-\alpha}$ is considered to be involved in the formation reaction of $Sr(NO_3)_2$ during the annealing of $SrZr_{0.9}Yb_{0.1}O_{3-\alpha}$ in the atmosphere containing NO and $O_2$.

### 3.2.3. Reaction of $SrCO_3$ with $NO_x$

One of the formation mechanisms of $Sr(NO_3)_2$ is considered to be the reaction of $SrCO_3$ with NO or $NO_2$, where $SrCO_3$ is the product of the reaction of $SrZrO_3$ with $CO_2$ as described in 3.2.1. This reaction may be written as Equations 27 and 28.

$$SrCO_3 + 2NO + 3/2O_2 \rightleftarrows Sr(NO_3)_2 + CO_2 \quad (27)$$

$$SrCO_3 + 2NO_2 + 1/2O_2 \rightleftarrows Sr(NO_3)_2 + CO_2 \quad (28)$$

Equations 29 and 30 are derived for reactions (27) and (28).

$$\text{Log } P_{NO} = 1/2 \text{ Log } P_{CO2} - 3/4 \text{ Log } P_{O2} + 10.92 - 8.68 \times 10^3/T \quad (29)$$

$$\text{Log } P_{NO2} = 1/2 \text{ Log } P_{CO2} - 1/4 \text{ Log } P_{O2} + 7.09 - 5.70 \times 10^3/T \quad (30)$$

By inserting $P_{O2} = 0.08$ into Equations 29 and 30, Equations 31 and 32 are obtained.

$$\text{Log } P_{NO} = 1/2 \text{ Log } P_{CO2} + 11.74 - 8.68 \times 10^3/T \quad (31)$$

$$\text{Log } P_{NO2} = 1/2 \text{ Log } P_{CO2} + 7.36 - 5.70 \times 10^3/T \quad (32)$$

Equations 31 and 32 are shown in Figs 11 and 12.

The concentration of $CO_2$ as an impurity in the gases used in this experiment is less than 2 ppm, i.e., $P_{CO2} < 2 \times 10^{-6}$, therefore, the experimental conditions belong to the region in which $Sr(NO_3)_2$ is stable.

In the case of reaction (2), $SrCO_3$ cannot exist at temperatures higher than 610 °C as shown in Fig. 4. As described in 3.2.1, $SrCO_3$ is considered to be formed at a temperature lower than 370 °C during cooling in

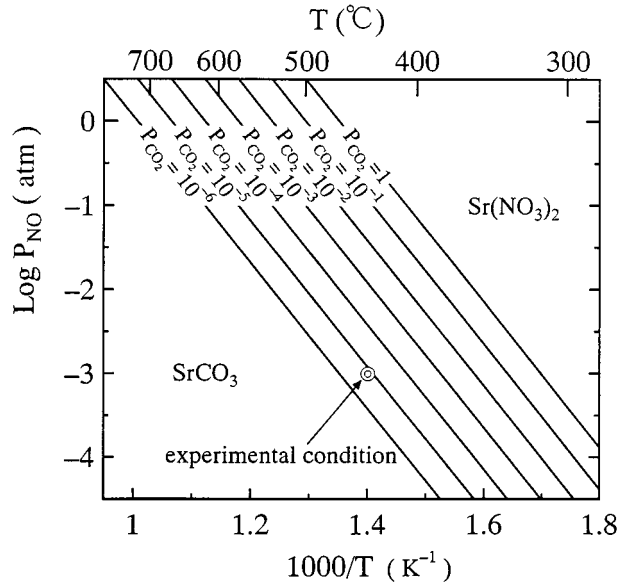


*Figure 11* Stability of $SrCO_3$ in atmosphere containing NO and 8% $O_2$.

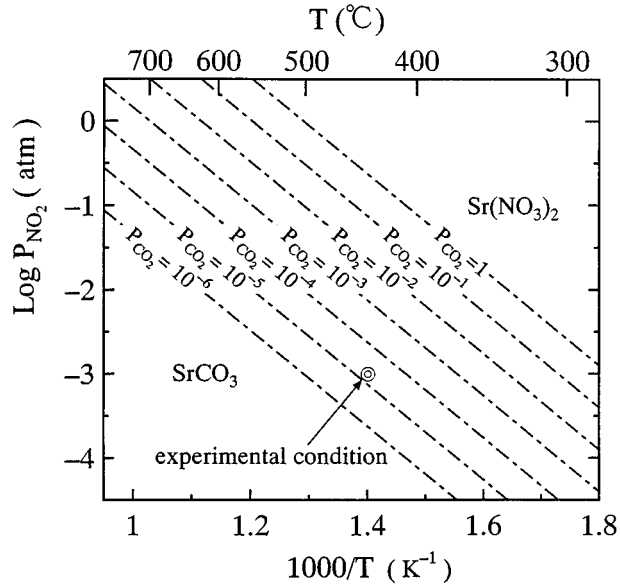


*Figure 12* Stability of $SrCO_3$ in atmosphere containing $NO_2$ and 8% $O_2$.

the first annealing in air or at room temperature before and after annealing. If $SrCO_3$ would be formed before annealing in the atmosphere containing NO and $O_2$, there is high possibility that $Sr(NO_3)_2$ is formed by the reaction of $SrCO_3$ with NO or $NO_2$.

It is not sure which mechanism is the main reaction for the formation of $Sr(NO_3)_2$. However, $SrZr_{0.9}Yb_{0.1}O_{3-\alpha}$ is not thermodynamically stable at a temperature lower than 500 °C and may decompose into $SrCO_3$ and $Sr(NO_3)_2$ by the reaction with $CO_2$ and $NO_x$. As described above, however, the reaction rate is significantly influenced by the characteristics of $SrZr_{0.9}Yb_{0.1}O_{3-\alpha}$. When a sintered $SrZr_{0.9}Yb_{0.1}O_{3-\alpha}$ with a small specific surface area is used as the electrolyte in electrical devices, the decomposition rate into $SrCO_3$ or $Sr(NO_3)_2$ is considered to be very slow. However, the formation of a small amount of $SrCO_3$ or $Sr(NO_3)_2$ is also considered to influence the electrical properties of $SrZr_{0.9}Yb_{0.1}O_{3-\alpha}$. Further studies on the rate of the decomposition reaction and the influence of the decomposition products on the characteristics of the electrolytes are necessary to realize the devices using $SrZr_{0.9}Yb_{0.1}O_{3-\alpha}$.

## 4. Conclusion

In order to investigate the stability of the $SrZr_{0.9}Yb_{0.1}O_{3-\alpha}$ protonic conductor in an atmosphere containing nitrogen oxides ($NO_x$), fine $SrZr_{0.9}Yb_{0.1}O_{3-\alpha}$ powder with a specific surface area of about 50 $m^2/g$ was annealed at 440 °C in He gas containing 8% $O_2$ and 0.1% NO. The formation of $Sr(NO_3)_2$ was observed by IR measurement, ion-chromatography analysis and ICP analysis. The reaction mechanism was examined by calculating the thermodynamic equilibrium. It is concluded that $H_2O$ dissolved into $SrZr_{0.9}Yb_{0.1}O_{3-\alpha}$ instead of $O_2$ in the atmosphere may play an important role in the reaction for the formation of $Sr(NO_3)_2$ between $SrZr_{0.9}Yb_{0.1}O_{3-\alpha}$ and $NO_x$.

## References


1. H. UCHIDA, H. YOSHIKAWA and H. IWAHARA, *Solid State Ionics* **34** (1989) 103.
2. H. UCHIDA, H. YOSHIKAWA, T. ESAKA, S. OHTSU and H. IWAHARA, *ibid.* **36** (1989) 89.
3. N. SATA, K. HIRAMOTO and M. ISHIGAME, *Physical Review B* **54** (1996) 15795.
4. W. MÜNCH, G. SEIFERT, K. D. KREUER and J. MAIER, *Solid State Ionics* **86–88** (1996) 647.
5. T. YAJIMA and H. IWAHARA, *ibid.* **53–56** (1992) 983.
6. *Idem., Sensors and Actuators B* **5** (1991) 145.
7. H. IWAHARA, H. UCHIDA, K. OGAKI and H. NAGATO, *J. Electrochem. Soc.* **138** (1991) 295.
8. T. YAJIMA, K. KOIDE, H. TAKAI, N. FUKATSU and H. IWAHARA, *Solid State Ionics* **79** (1995) 333.
9. N. KURITA, N. FUKATSU, S. MIYAMOTO, F. SATO, H. NAKAI, K. IRIE and T. OHASHI, *Metall. Mater. Trans. B* **27** (1996) 929.
10. N. FUKATSU, N. KURITA, T. OHASHI and K. KOIDE, *Solid State Ionics* **113–115** (1998) 219.
11. H. IWAHARA, H. UCHIDA and S. TANAKA, *ibid.* **9/10** (1983) 1021.
12. *Idem., J. Appl. Electrochem.* **16** (1986) 663.
13. H. IWAHARA, T. YAJIMA, T. HIBINO and H. USHIDA, *J. Electrochem. Soc.* **140** (1993) 1687.
14. H. IWAHARA, T. YAJIMA and H. USHIDA, *Solid State Ionics* **70/71** (1994) 267.
15. N. TANIGUCHI, E. YASUMOTO and T. GAMO, *J. Electrochem. Soc.* **143** (1996) 1886.
16. S. HAMAKAWA, T. HIBINO and H. IWAHARA, *ibid.* **140** (1993) 459.
17. *Idem., ibid.* **141** (1994) 1720.
18. T. HIBINO, S. HAMAKAWA, T. SUZUKI and H. IWAHARA, *J. Appl. Electrochem.* **24** (1994) 126.
19. T. KOBAYASHI, S. MORISHITA, K. ABE and H. IWAHARA, *Solid State Ionics* **86–88** (1996) 603.
20. N. TANIGUCHI and T. GAMO, *Denki Kagaku* **62** (1994) 326.
21. M. J. SCHOLTEN, J. SCHOONMAN, J. C. MILTENBURG and H. A. J. OONK, The Electrochem. Soc. 183rd Meeting (Honolulu) Vol. 93 No. 1 (1993) p. 1625.
22. M. J. SCHOLTEN, J. SCHOONMAN, J. C. MILTENBURG and H. A. J. OONK, *Solid State Ionics* **61** (1993) 83.
23. K. D. KREUER, *ibid.* **97** (1997) 1.
24. *Idem., ibid.* **125** (1999) 285.



*Received 16 November 1999*
*and accepted 4 April 2000*